

# Temperature-dependent composition, ordering, and band bending at GaP(100) surfaces

I. M. Vitomirov, A. Raisanen, and L. J. Brillson  
*Xerox Webster Research Center, Webster, New York 14580*

C. L. Lin, D. T. McInturff, P. D. Kirchner, and J. M. Woodall  
*IBM T. J. Watson Research Center, Yorktown Heights, New York 10598*

(Received 28 December 1992; accepted 12 April 1993)

We have used soft x-ray photoemission spectroscopy (SXPS), Auger electron spectroscopy (AES), and low-energy electron diffraction (LEED) to investigate thermally induced changes in atomic composition, bonding, and geometric ordering at GaP(100) surfaces prepared by molecular-beam epitaxy. Following growth, GaP(100) surfaces were coated with several monolayers of P, after which an  $\sim 2000$  Å-thick As cap was applied to seal the structure for transfer to analytical chambers. Surface-sensitive SXPS core-level spectra and more bulk-sensitive AES spectra collected at *in situ* annealed surfaces indicate complex changes in P, As, and Ga atomic ratios throughout the 350–650 °C desorption temperature range. Core-level photoemission intensity ratios reveal rapid loss of both P and As for surface annealing temperatures below 450 °C, a dramatic increase (decrease) in the P (As) concentration in the 450–550 °C range, and a relatively stable, stoichiometric GaP(100) surface composition for temperatures between  $\sim 550$  and 640 °C, above which thermally driven surface decomposition becomes noticeable. Existence of clear LEED patterns,  $(1 \times 2)$  for desorption temperatures below  $\sim 450$  °C and  $(4 \times 2)$ - $c(8 \times 2)$  above this temperature, indicates little sensitivity of GaP(100) surface reconstructions to details of surface stoichiometry and bonding. We propose that both this insensitivity and the abrupt changes in the P to As atomic ratios indicate strong competition between the two anions to form bonds with Ga surface atoms. In this context, compositional and structural details of decapped GaP(100) depend sensitively on the interplay of surface desorption, atomic diffusion from the substrate to the free surface, and the anion-cation chemical bonding at the surface. Overall, our work demonstrates the success of As and P capping combined with subsequent thermal desorption in producing stable GaP(100) surfaces with desired chemical and electronic properties.

## I. INTRODUCTION

Single-crystal GaP is a material of high technological importance, primarily because of its use in red, orange, yellow, and green light emitting diodes (LEDs).<sup>1,2</sup> It also represents a useful substrate for the growth of ordered heterostructure and quantum well devices.<sup>3,4</sup> In addition to its technological applications, the (100) surface of GaP exhibits a number of scientifically intriguing properties. In analogy to GaAs(100), the structural and physical properties of GaP(100) are significantly affected by its atomic composition.<sup>5–10</sup> However, unlike GaAs(100) which exhibits several surface reconstructions throughout its composition range,<sup>5–9</sup> surface reconstructions reported for GaP(100) include only the P-stabilized  $(1 \times 2)$  and the Ga-stabilized  $(4 \times 2)$  reconstructions.<sup>2,10</sup> It is both important and interesting to understand the physical mechanisms responsible for this difference, as well as to establish precise conditions under which GaP(100) surface ordering may be accomplished. Furthermore, establishing a methodology for producing clean and ordered GaP(100) surfaces in ultrahigh vacuum opens new possibilities for the investigation of Schottky barrier evolution mechanisms on polar III–V semiconductor surfaces.<sup>11,12</sup>

In the present article we describe an *in situ* surface preparation procedure which results in clean GaP(100) sur-

faces with controllable surface composition, ordering, and electronic properties. The procedure involves in-vacuum thermal desorption of As and P protective layers from GaP(100) surfaces grown by molecular-beam epitaxy (MBE) and As and P capped prior to removal from the growth chamber. We use core-level and valence-band soft x-ray photoemission (SXPS) in conjunction with detailed line shape analysis to study changes in surface bonding and atomic ratios between the Ga, P, and adsorbed As atomic species as a function of surface annealing temperature. In addition, we use a more bulk-sensitive Auger electron spectroscopy (AES) to monitor composition changes in the region tens of angstroms below the surface, as well as to verify the absence of C and O contaminants on the surface. The low-energy electron diffraction (LEED) patterns which we obtain include a  $(1 \times 1)$  pattern for a 350 °C annealed surface, a  $(1 \times 2)$  pattern for the 350–425 °C annealing temperature range, and a  $(4 \times 2)$ - $c(8 \times 2)$  pattern for anneals between 450 and 640 °C. The transition between the anion-terminated  $(1 \times 2)$  and the Ga-terminated  $c(8 \times 2)$  surface reconstructions occurs within a very narrow ( $\sim 20$  °C) temperature range. However, each of the two LEED patterns becomes better defined and sharper with both increasing temperature and the duration of annealing within its characteristic range of temperatures.

This trend, in analogy with our previous observations at annealed GaAs(100) surfaces, appears to indicate an improvement in surface ordering and homogeneity with the duration of surface annealing.<sup>9</sup> However, secondary electron photoemission spectra near cutoff demonstrate the existence of varying degrees of surface patchiness throughout the range of desorption temperatures.<sup>9</sup> The surface Fermi level ( $E_F$ ), measured by both the valence-band edge extrapolation and rigid shifts in core levels, spans the range from 0.78 to 1.03 eV above the valence-band maximum ( $E_v$ ) as a function of surface reconstruction and/or composition. This range of positions agrees very well with the measured deep level energy distribution at these surfaces and reveals the sensitivity of the electronic properties of clean GaP(100) surfaces to the details of surface bonding, composition, and geometry.<sup>13</sup>

## II. EXPERIMENT AND DATA ANALYSIS

We carried out SXPS experiments at the Synchrotron Radiation Center of the University of Wisconsin using a 6 m toroidal grating monochromator (TGM) and beamline. Measurements were performed in an ultrahigh vacuum stainless-steel chamber equipped with a double-pass cylindrical mirror energy analyzer (CMA), LEED, and a setup for thermal desorption of As and P surface coatings. We excited Ga 3*d*, P 2*p*, and As 3*d* core-level spectra with 80, 170, and 100 eV photons, respectively, and we monitored the valence-band (VB) emission at 47 eV incident photon energy. Photoemission measurements of the secondary electron near-cutoff structure and surface ionization energy were carried out using 22 eV photons and with a negative (−7 V) sample bias relative to the analyzer ground. Surface ionization energy can thus be derived from the energy separation between the top of the valence-band edge and the low-energy cutoff of the secondary electron emission, both determined by linear extrapolation of the spectral edge to the background emission.<sup>9,14,15</sup>

Core-level photoemission spectra were analyzed in terms of Gaussian-broadened Lorentzians using a standard nonlinear least-squares line-shape fitting routine.<sup>9,16</sup> Lorentzian widths (defined as a full width at half maximum) were optimized from a number of fits and subsequently fixed at 155 meV for the Ga 3*d*, 180 meV for the As 3*d*, and 150 meV for the P 2*p* spectra. Spin-orbit splitting and branching ratio were also held constant for each core level, with the spin-orbit split values of 445, 690, and 860 meV corresponding to the Ga 3*d*, As 3*d*, and P 2*p* levels, respectively. The remaining parameters, i.e., the Gaussian width, kinetic energy, intensity, and branching ratio, were allowed to vary freely in the fitting procedure, but they were monitored for self-consistency between different surface reconstructions and compositions. In analogy with the fitting procedure described in Refs. 9 and 17 for decapped GaAs(100) surfaces, we maintained equal branching ratios and Gaussian widths between the substrate and the surface-shifted components of the Ga 3*d* and P 2*p* spectra.

The *n*-type Si-doped ( $N_d = 3 \times 10^{17} \text{ cm}^{-3}$ ) GaP(100) surfaces were prepared at the IBM T. J. Watson Research

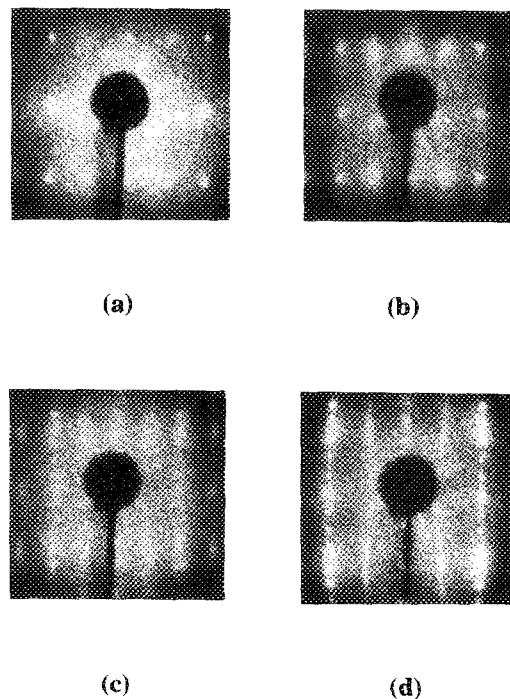


FIG. 1. Representative LEED spectra from decapped GaP(100) surfaces: (a) (1×1) at 350 °C; (b) (1×2) at 425 °C; (c) (4×2)-c(8×2) at 450 °C; (d) (4×2)-c(8×2) at 600 °C. All spectra were assessed after a 5 min surface anneal at a designated temperature and with electron beam energies of 75–77 eV.

Center by MBE growth on top of chemically etched, S-doped GaP(100) substrates. Before removal from the MBE chamber, the surfaces were encapsulated with several layers of P, on top of which a thick (>2000 Å) film of amorphous As was deposited. The specimens were then shipped to the Xerox Webster Research Center under vacuum. We obtained GaP(100) surfaces free of oxygen and carbon contamination by thermal desorption of As and P in vacuum chambers equipped with ion and cryogenic pumps (base pressure  $\sim 10^{-10}$  Torr). We performed desorptions in multiple steps, each one at a gradually increased temperature. Two types of annealing cycles were used: one consisting of 5 min anneals at a desired temperature, and the other involving a nearly linear temperature ramp ( $\sim 5\text{--}10$  °C/s) with a  $\sim 5$  s anneal at the maximum temperature. Following annealing, the sample was allowed to cool down and the measurements were carried out at the ambient temperature.

## III. RESULTS AND DISCUSSION

In Fig. 1 we show representative LEED patterns observed at *in situ* decapped GaP(100) surfaces. Annealing the surface to  $\sim 350$  °C produces a diffuse (1×1) pattern shown in Fig. 1(a), which also contains weak diffraction spots suggestive of a nascent (1×2) surface reconstruction. Upon annealing to this temperature, most of the As and P protective layer is removed. This process was visually accompanied by “defogging” of the specimen surface, which changed from a dull gray to a deep orange color. However, SXPS measurements reveal the presence of at

least a couple of monolayers of both the weakly physisorbed As and P at this surface, in good agreement with the As desorption behavior observed at decapped GaAs(100) surfaces.<sup>9,17</sup> For annealing temperatures between  $\sim 350$  and  $\sim 425$  °C, we observed the  $(1 \times 2)$  LEED pattern which becomes sharper with increasing annealing temperature [Fig. 1(b)]. This surface reconstruction, corresponding to an anion-terminated surface, has been previously reported by van Bommel and Crombeen, who produced it at a sputtered-and-annealed GaP(100) surfaces exposed to  $10^{-5}$  Torr  $\text{PH}_3$  overpressure.<sup>10</sup> In contrast, Baillargeon, Cheng, and Hsieh observed a  $(2 \times 4)$  P-terminated surface structure during the gas-source MBE growth of GaP(100).<sup>2</sup> These different surface reconstructions of P-terminated GaP(100) may reflect the sensitivity of the surface reconstruction to the details of P incorporation process in post-growth versus in-growth processing. In addition, as we discuss later in this article, the bonding configuration at our decapped surfaces is further complicated by the simultaneous presence of P and As atomic species at the surface, both of which have an affinity to form a bond with subsurface Ga atoms.

In the temperature range between  $\sim 425$  and  $450$  °C, we observe an abrupt transition from a sharp  $(1 \times 2)$  to a well-defined  $(4 \times 2)$ - $c(8 \times 2)$  LEED pattern [Fig. 1(c)]. This transition corresponds to the change from an anion to the Ga-dimer surface termination.<sup>2,10</sup> The  $(4 \times 2)$ - $c(8 \times 2)$  surface reconstruction, in analogy with the same reconstruction observed at GaAs(100) surfaces, persists over a wide range of annealing temperatures and starts to deteriorate only as incipient surface decomposition begins to take place at temperatures approaching  $\sim 650$  °C (as compared to  $\sim 620$  °C for GaAs). We speculate that this surface reconstruction for GaP(100) originates from a missing Ga dimer at the Ga-terminated surface, in direct analogy with the scanning tunneling microscopy results obtained at GaAs(100) surfaces.<sup>18,19</sup> With increasing desorption temperature, as well as the duration of the anneals between  $450$  and  $620$  °C, the  $c(8 \times 2)$  LEED pattern becomes gradually sharper, as shown in Fig. 1(d). Interestingly, we find the  $c(8 \times 2)$  LEED pattern on GaP(100) generally sharper and stable over a wider range of temperatures than in the case of As-capped and annealed GaAs(100) surfaces. This is possibly due to the higher Ga-P bond strength relative to Ga-As, with their respective bulk heats of formation being  $-88$  and  $-71$  kJ/mol.<sup>20</sup> In addition, both the SXPS and AES measurements indicate that large variations in the P to As atomic ratios take place in the temperature range corresponding to the  $c(8 \times 2)$  surface reconstruction. The insensitivity of the  $c(8 \times 2)$  surface reconstruction to the changes in the relative anion concentration at the surface may be due to the insensitivity of the surface geometry to the bonding details between the Ga dimers and the anions in the second layer (P, As, or both). However, this insensitivity may also be due to the insensitivity of the LEED technique itself to the possible presence of disordered P and As patches on the surface which could cause the observed variations in surface composition.

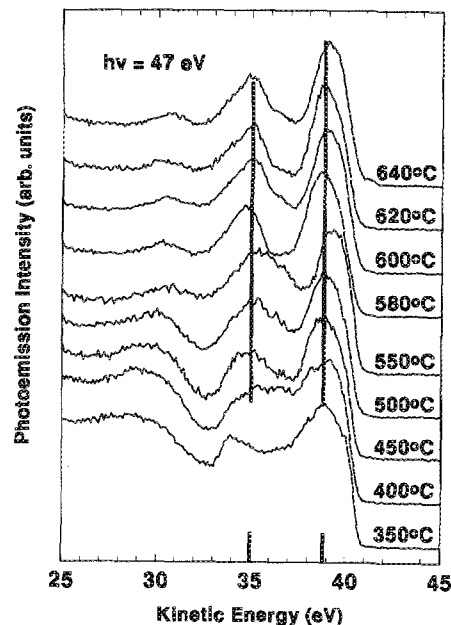


FIG. 2. GaP(100) valence-band spectra show minor and gradual changes with surface annealing temperatures below  $\sim 580$  °C, and virtually no change above this temperature. The changes mainly occur in the relative prominence of the peaks at 35 and 38.8 eV kinetic energies, marked with the vertical lines in the figure.

Figure 2 shows valence-band photoemission spectra representative of decapped GaP(100) surfaces. These spectra, taken at 47 eV photon energy and normalized to the same height, undergo gradual changes with annealing temperature in the  $350$ – $450$  °C temperature range. The spectral shape changes as the feature at  $\sim 35$  eV kinetic energy becomes sharper and more pronounced relative to the highest kinetic-energy feature at  $\sim 38.8$  eV. Both of these features are highlighted with vertical bars in Fig. 2. The changes in the valence-band emission parallel the transition in surface reconstruction from the anion-terminated  $(1 \times 1)$  and  $(1 \times 2)$  to the more Ga-rich  $(4 \times 2)$ - $c(8 \times 2)$  surface geometry. Furthermore, gradual evolution of the valence-band features continues for desorption temperatures between  $450$  and  $580$  °C, which indicates significant changes in surface composition and/or morphology in spite of the same well-defined  $c(8 \times 2)$  LEED pattern. For desorption temperatures  $\geq 580$  °C neither the surface LEED pattern nor valence-band emission exhibit any further changes with temperature, which is consistent with the existence of a relatively stable and stoichiometric GaP(100)  $c(8 \times 2)$  surface in this temperature range. Only the topmost valence-band spectrum in Fig. 2, which corresponds to the  $640$  °C annealed surface, displays a shoulder at the high kinetic-energy end of the spectrum. Based on the simultaneous changes which occur in the Ga  $3d$  core-level spectra in this temperature range, we associate the new emission with metallic states produced by Ga clusters on the surface.

Valence-band spectra in Fig. 2 also provide an indication of the surface  $E_F$  position (not shown) at decapped GaP(100) surfaces. Our results, based on the combined

valence-band edge and core-level shift analysis,<sup>9</sup> indicate that the  $E_F$  at P- and As-capped GaP(100) stabilizes  $\sim 0.8$  eV above the valence-band maximum ( $E_v$ ) for highly As- and P-rich surfaces annealed to below  $\sim 400^\circ\text{C}$ . Thermal desorptions in the  $450\text{--}550^\circ\text{C}$  temperature range move the Fermi level to  $\sim 1.0$  eV above  $E_v$ . For desorption temperatures between  $550$  and  $620^\circ\text{C}$  and the Ga-dimer stabilized stoichiometric  $c(8\times 2)$  surface, the  $E_F$  stabilizes at a new position  $\sim 0.9$  eV above  $E_v$ . The  $(E_F - E_v)$  hence spans the range from  $\sim 0.8$  to  $\sim 1.0$  eV at decapped GaP(100) surfaces. This movement of the surface Fermi level as a function of surface composition and/or reconstruction underlines the sensitivity of the surface electronic structure to its chemical composition and bonding. In addition, this movement emphasizes the lack of strong surface "pinning" and suggests decapped GaP(100) as a useful substrate for the Schottky barrier studies.

Figure 3(a) shows surface sensitive Ga  $3d$  spectra taken at  $80$  eV incident photon energy (estimated escape depth of  $\sim 5$  Å).<sup>21</sup> In close analogy with the Ga  $3d$  spectra from decapped GaAs(100) surfaces, the line-shape decomposition of these spectra shows the presence of the substrate Ga  $3d$  component (1) and of two surface-shifted components, (2) and (3), at the high and low binding energy side of the substrate, respectively.<sup>9</sup> In contrast to GaAs(100) surfaces, for which the relative binding energies of the surface-shifted components showed systematic variations with the annealing temperature, the surface shifts of components (2) and (3) for GaP(100) remain stable at  $0.46 \pm 0.04$  eV and  $0.55 \pm 0.04$  eV throughout the  $400\text{--}620^\circ\text{C}$  range of annealing temperatures. Larger deviations in surface-shifted component energies from these values were observed only at the extremes of the annealing temperature range, corresponding to the As- and P-covered  $(1\times 1)$  surface after a  $350^\circ\text{C}$  desorption (spectrum now shown), and to the slightly decomposed surface annealed to  $640^\circ\text{C}$  [Fig. 3(a), top spectrum]. The latter surface also shows a well-defined new feature (4) at the lowest binding energy relative to the substrate, which is attributed to the formation of metallic Ga clusters at the decomposed portions of the surface. In contrast to the relatively minor changes in the surface-shifted component binding energies relative to the substrate, Fig. 3(a) shows a large and systematic change in the relative intensity of the two surface-shifted components in the Ga  $3d$  spectra at annealed GaP(100) surfaces. For desorption temperatures between  $400$  and  $500^\circ\text{C}$ , component (2) contributes  $\sim 25\%$  of the total Ga  $3d$  line emission, whereas component (3) contributes only  $\sim 5\%$ – $7\%$  of the total emission intensity in the same temperature range. Conversely, for higher desorption temperatures between  $580$  and  $620^\circ\text{C}$ , component (2) contributes less than  $\sim 1\%$  of the total emission intensity (meaning that it is *de facto* absent from the Ga  $3d$  spectra), whereas the component (3) contribution is stabilized at its maximum value of  $\sim 21\%$ . For temperatures between these two characteristic regions, a gradual attenuation of component (2) and a complementary enhancement of surface shifted component (3) is observed. Significantly, these highly reproducible variations in the Ga  $3d$  line shape with surface anneal-

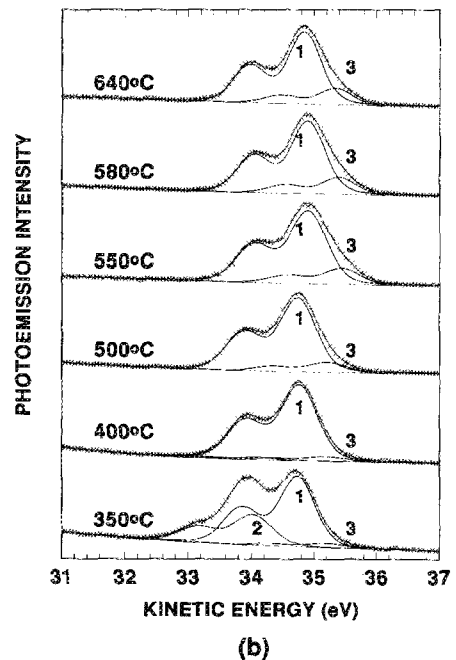
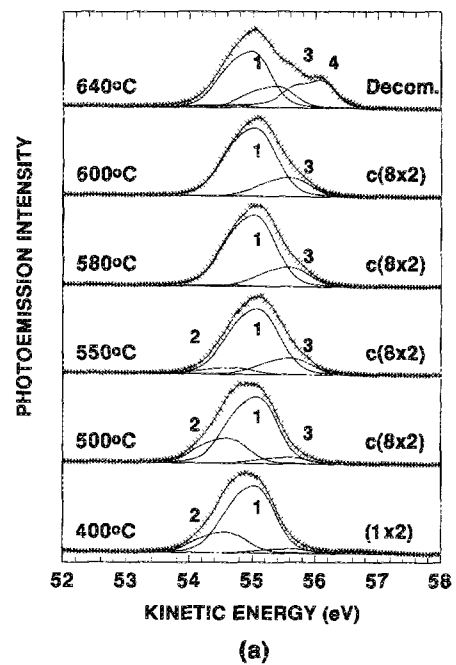


FIG. 3. Effect of desorption temperature induced changes in surface composition and reconstruction on (a) Ga  $3d$  and (b) P  $2p$  surface sensitive photoemission spectra for clean GaP(100). Ga  $3d$  core levels show the substrate (1) and two surface shifted components, (2) and (3), while there is only a single surface shifted component in the P  $2p$  spectra (3). Incipient surface decomposition produces a distinct component (4) at the low binding energy side of the Ga  $3d$  emission.

ing temperature and/or composition are observed within the temperature range of a single,  $c(8\times 2)$ , GaP(100) surface reconstruction. It is thus unlikely that the two surface-shifted components may be assigned to differently positioned Ga dimers within the  $(4\times 2)$  surface unit cell.<sup>17</sup> In agreement with our recent observations at decapped GaAs(100) surfaces, the two components possibly reflect the relative concentration of As at the surface.<sup>9</sup> In that

case, an As-rich environment would give rise to a prominent surface-shifted component (2) at the high binding energy side of the substrate, whereas an As-deficient (and P-rich) surface would result in a complete absence of component (2) and a dominant presence of surface shifted component (3) at the low binding energy side of the spectrum.

The surface-sensitive P 2*p* core-level spectra, shown in Fig. 3(b), undergo fewer changes with desorption temperatures than do their Ga 3*d* counterparts. The bottom spectrum in Fig. 3(b), obtained after a 5 min desorption at 350 °C, comprises a substrate component (1), a component (2) shifted 0.70 eV to higher binding energies, and a very weak (~4% of the total intensity) component (3) shifted -0.48 eV in binding energy relative to the substrate. Subsequent desorption to 450 °C results in a tenfold decrease in the relative emission intensity of component (2), which for this desorption temperature contributes only ~3% of the total P 2*p* emission intensity. Its rapid attenuation with annealing and its chemical shift to higher binding energies lead us to assign component (2) to a relatively weakly physisorbed P capping layer at the surface. Component (3) increases in intensity relative to the substrate (1) for desorption temperatures between 350 and 550 °C, after which it saturates at ~18% of the total emission intensity. In analogy with decapped GaAs(100) surfaces, feature (3) is hence identified as a surface shifted component (-0.49 ± 0.02 eV shift relative to the substrate) which is indicative of a different bonding environment of P atoms at or near the Ga-dimer terminated *c*(8×2) surface.<sup>9,17</sup> The constant P 2*p* line shape for anneals above 550 °C agrees very well with our previous observations regarding the Ga 3*d* and valence-band spectra in this temperature range. Along with the LEED pattern which also shows no change in this temperature range, these results suggest that we are able to produce stable and stoichiometric GaP(100) *c*(8×2) surfaces for *in vacuo* desorption temperatures between 550 and 640 °C.

Understanding temperature-dependent composition changes of decapped GaP(100) surfaces requires simultaneous monitoring line shapes as well as emission intensities of the Ga 3*d*, P 2*p*, and As 3*d* core levels. In Fig. 4 we plot ratios between the total emission intensities of these core levels as a function of annealing temperature. Integrated intensities were obtained after subtraction of a cubic polynomial background and were subsequently normalized to their respective ionization cross sections.<sup>22</sup> The As 3*d*/Ga 3*d* ratio decreases monotonically from ~2.34 at 350 °C to ~0.06 at 550 °C, and then saturates between 0.03 and 0.04 for temperatures between 580 and 640 °C. This residual As, equivalent to several hundredths of a monolayer surface coverage, exhibits a strong affinity for the Ga-terminated GaP(100) surface and cannot be removed at temperatures below the GaP(100) surface decomposition temperature. Indeed, analysis of the As 3*d* spectra (not shown) reveals a nearly constant As 3*d* line shape for desorption temperatures ≥ 550 °C. The line shape is comprised of two spectral components, which indicates that chemisorbed As atoms

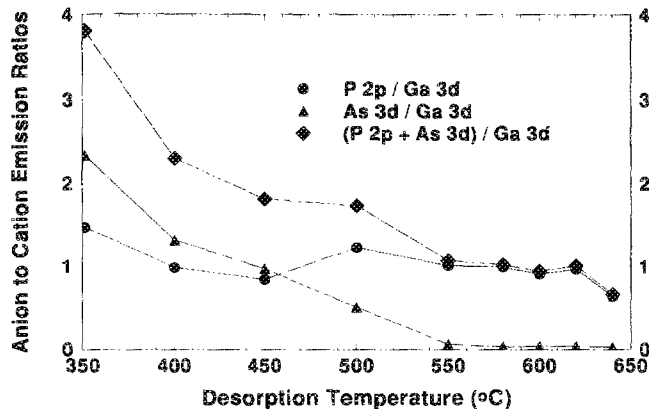


FIG. 4. Total emission intensity ratios between the P 2*p* and Ga 3*d* spectra (circles), and between the As 3*d* and Ga 3*d* core-level spectra (triangles) as a function of the GaP(100) surface annealing temperature. As is continuously desorbed from the surface below 550 °C while P remains on the surface as a result of the outdiffusion from the substrate. Dashed line indicates the total anion (P 2*p* + As 3*d*) emission normalized to the Ga 3*d* signal intensity.

occupy two inequivalent bonding sites at the *c*(8×2) reconstructed GaP(100) surface.

While the As 3*d*/Ga 3*d* ratio decreases monotonically for desorption temperatures below 550 °C, the P 2*p*/Ga 3*d* ratio in Fig. 4 undergoes dramatic changes in the same temperature range: it starts off at ~1.5 for the 350 °C annealed surface, reaches a minimum of ~0.84 at the 450 °C annealed surface, and then rises again toward its stoichiometric value (defined as ~1.0) which it attains upon a 550 °C anneal. The initial decrease in both the P 2*p* and As 3*d* emission intensities relative to the Ga 3*d* emission with annealing may be directly associated with the thermal desorption of the P and As protective coating from the GaP surface.<sup>23</sup> Interestingly, since both the P vapor pressure and the P desorption rate from a clean GaP(100) surface are higher than the As vapor pressure and desorption rate from a GaAs(100) surface, one might expect a faster removal of the P protective layer relative to that of the As cap on our surfaces.<sup>23</sup> However, the results in Fig. 4 indicate that the initial As removal (for desorption temperatures < 450 °C) is faster than that of P. This is likely caused by the geometry of our protective coating (As atop of P), as well as by the fact that in our case the As layer is adsorbed on top of the P layer rather than the GaAs surface. Furthermore, the subsequent increase in the P 2*p*/Ga 3*d* ratio for temperatures between 450 and 550 °C cannot be explained in terms of the P desorption process alone. This increase may be due to the thermally driven P diffusion from the GaP substrate toward the free surface. Indeed, our AES measurements of decapped GaP(100) surfaces, which have a higher probe depth than the SXPS measurements, also indicate a relative P enrichment of the surface for annealing temperatures above ~450 °C. Then, the relatively stable stoichiometry of the *c*(8×2) GaP(100) surface in the 550–620 °C temperature range must be maintained through a delicate balance between the P diffusion from the bulk to the surface and the P desorp-

tion (and possibly readsorption) from the surface into the vacuum. It is also conceivable that both of these processes may be affected by the geometric structure and chemical bonding in the topmost layers of the surface, and that the reconstructed surface itself acts as a moderator of the thermally stimulated atomic transport across the GaP/vacuum interface.

At this point we can also offer several remarks regarding our GaP(100) surface preparation technique. In comparison with the thermally decapped GaAs(100), the ratio between the total anion ( $P\ 2p + As\ 3d$ ) and the  $Ga\ 3d$  photoemission signal intensities, shown in Fig. 4, undergoes gradual changes which are similar to the  $As\ 3d/Ga\ 3d$  ratio variations at As-capped and *in situ* annealed GaAs(100) surfaces.<sup>9</sup> This indicates that the simultaneous presence of both the P and As anions at decapped GaP(100) possibly results in a competition between the two anions to form bonds with surface Ga atoms, but that these anion exchange reactions do not have a negative impact on the GaP surface stability and ordering. On the contrary, the quality of LEED patterns suggests that decapped GaP(100) surfaces are better ordered and less affected by either the length of the annealing cycles or by the vacuum condition in the chamber. Furthermore, we observe analogous surface atomic ratio and core-level evolution trends with desorption temperature between the surfaces prepared by rapid thermal annealing cycles (ramp to a desired temperature followed by quenching) and those using 5 min anneals at a desired temperature. The only difference between the two types of surface preparation techniques is that the transition temperatures between different surface regimes are shifted systematically to higher values for rapid anneal cycles. This is to be expected since rapid anneals do not allow the surface to fully achieve its equilibrium atomic distribution at a given temperature. This difference is confirmed by the secondary electron photoemission spectra near the low-energy cutoff which show higher variations in the near-cutoff features for rapidly annealed surfaces. As discussed by Ranke, the multiple features near the cutoff are indicative of the presence of different work function phases on a surface, and therefore serve as a fingerprint of surface inhomogeneity.<sup>9,14</sup>

In Fig. 5 we schematically summarize our analysis of the evolution of decapped GaP(100) surfaces *in situ* annealing. Upon a 350 °C anneal, the bulk of the As cap is removed from the surface which is still covered with a couple of monolayers of As and/or P. Photoemission results in Fig. 4 indicate that for this annealing temperature there is ~50% more As than P coverage at the surface. This might be due either to the preferential thermal removal of the P interlayer (in which case As would be in direct contact with a large portion of the GaP surface), or to the fact that As stays on top of the thin P film and thereby attenuates the  $P\ 2p$  signal. The surface exhibits a diffuse ( $1\times 1$ ) LEED pattern and a weak indication of a ( $1\times 2$ ) reconstruction, possibly arising from exposed surface patches with a reduced anion composition. Annealing between 350 and 425 °C results in a gradual improvement (sharpening and increased contrast) of the ( $1\times 2$ ) LEED

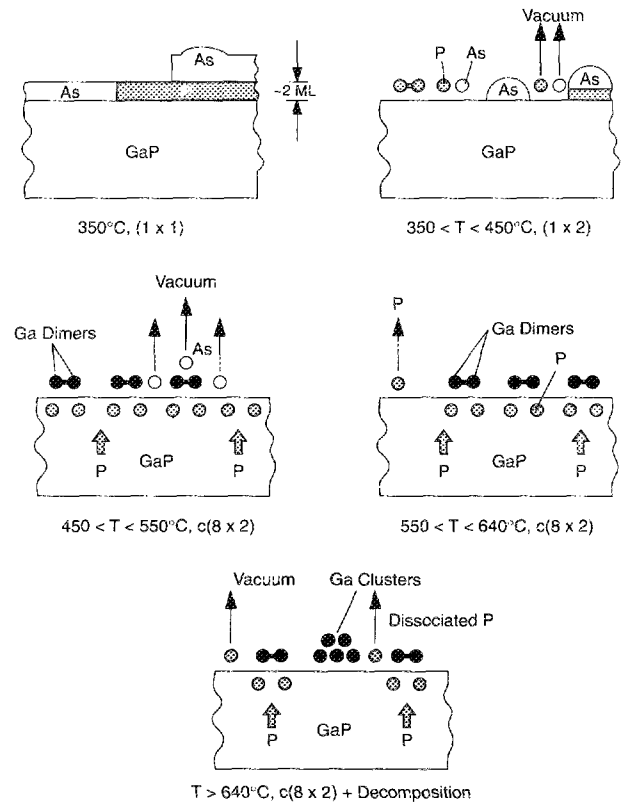


FIG. 5. Schematic of the atomic distributions and transport across the surface at decapped GaP(100) surfaces as a function of surface annealing temperature.

pattern due to the increased exposure of P and/or As terminated GaP surface. The ( $1\times 2$ ) surface reconstruction corresponds to the GaAs(100) ( $2\times 4$ )- $c(2\times 8)$  reconstruction in terms of the effective anion coverage of ~0.75 monolayers (ML).<sup>9</sup> Photoemission spectra indicate complete removal of both weakly physisorbed P and As species in this temperature range. Although the P desorption is expected to exceed As loss in this temperature range because of the higher P vapor pressure, it is probably kinetically limited by the presence of As coating. Nevertheless, the atomic ratios in Fig. 4 indicate that at ~450 °C the surface becomes P deficient and nearly stoichiometric in terms of the  $As\ 3d/Ga\ 3d$  ratio. For desorption temperatures between 450 and 550 °C, the LEED pattern abruptly switches from ( $1\times 2$ ) to ( $4\times 2$ )- $c(8\times 2)$  symmetry indicating that the GaP(100) surface is terminated with ordered Ga dimers. The  $c(8\times 2)$  LEED pattern becomes increasingly sharp in this temperature range as both the P and As atoms continue to be desorbed from the surface. However, while the As loss from the surface proceeds continuously due to the thermal removal of the As cap, the P to Ga ratio begins to rise again. The increase in the P surface concentration requires a new supply of phosphorus atoms and we speculate that such supply is provided by the thermally activated P diffusion from the substrate. In the temperature range between 550 and ~640 °C, there is a limited steady-state flow of P across the interface as the surface achieves its optimum Ga dimer-terminated geom-

etry through the balance of P supply from the substrate and its desorption from the surface. The LEED pattern retains its sharpness and all the core-level and valence-band photoemission spectra remain unchanged. The presence of As on the surface is reduced to several hundredths of a monolayer, which is possibly chemically bonded to defect sites on the surface. Finally, at temperatures below  $\sim 640^\circ\text{C}$ , incipient surface decomposition takes place. This decomposition accelerates at even higher temperatures and results in the removal of dissociated P atoms and the formation of Ga agglomerates at the surface, observed via valence-band and core-level SXPS spectra.

#### IV. CONCLUSIONS

Surface-sensitive SXPS core-level spectra and more bulk-sensitive AES spectra collected at *in situ* annealed GaP(100) surfaces indicate complex but systematic changes in the P, As, and Ga atomic ratios throughout the  $350\text{--}650^\circ\text{C}$  desorption temperature range. The existence of clear LEED patterns, the  $(1\times 2)$  for desorption temperatures below  $\sim 450^\circ\text{C}$  and the  $(4\times 2)\text{-}c(8\times 2)$  above this temperature, indicates little sensitivity of the GaP(100) surface reconstructions to details of surface stoichiometry and bonding. We propose that this insensitivity may be partially due to the strong competition between the two anions to form bonds with surface Ga, and that a well-ordered anion-terminated surface may result from either As or P bonding to Ga. The Ga-rich  $c(8\times 2)$  surface reconstruction is optimized upon a nearly complete removal of surface As and possibly acts as a moderator of the P transport across the free surface. Surface  $E_F$  lies 0.8 eV above  $E_v$  for the more Ga-rich surfaces annealed to between  $550$  and  $620^\circ\text{C}$ , and 1.0 eV above  $E_v$  for the more anion-rich surfaces in the  $400$  and  $450^\circ\text{C}$  desorption temperature range. Our work reveals the dependence of structural, chemical, and electronic properties of GaP(100) on the specifics of surface processing. It also demonstrates that *in situ* thermal decapping can be utilized to produce stable MBE GaP(100) surfaces with desirable structural and electronic properties.

#### ACKNOWLEDGMENTS

The authors wish to acknowledge the assistance of the SRC Staff in photoemission work performed at the Synchrotron Radiation Center of the University of Wisconsin-Madison, an NSF-supported facility. This work was in part supported by the Office of Naval Research under Contract No. N00014-91-C-0037.

- <sup>1</sup>E. W. Williams and R. Hall, *Luminescence and the Light Emitting Diode* (Pergamon, Oxford, 1978).
- <sup>2</sup>J. N. Baillargeon, K. Y. Cheng, and K. C. Hsieh, *Appl. Phys. Lett.* **56**, 2201 (1990).
- <sup>3</sup>T. Nomura, K. Murakami, K. Ishikawa, M. Miyao, T. Yamaguchi, A. Sasaki, and M. Hagino, *Surf. Sci.* **242**, 166 (1991).
- <sup>4</sup>W. Jiang, G. Zhou, K. Chen, C. Sheng, X. Zhang, and X. Wang, *Appl. Phys. Lett.* **51**, 1910 (1987).
- <sup>5</sup>A. Y. Cho, *J. Appl. Phys.* **47**, 2841 (1976).
- <sup>6</sup>R. Ludeke and A. Koma, *J. Vac. Sci. Technol.* **13**, 241 (1976).
- <sup>7</sup>J. Massies, P. Devoldère, and N. T. Linh, *J. Vac. Sci. Technol.* **15**, 1353 (1979).
- <sup>8</sup>R. Z. Bachrach, R. S. Bauer, P. Chiaradia, and G. V. Hansson, *J. Vac. Sci. Technol.* **19**, 335 (1981).
- <sup>9</sup>I. M. Vitomirov, A. Raisanen, A. C. Finnefrock, R. E. Viturro, L. J. Brillson, P. D. Kirchner, G. D. Pettit, and J. M. Woodall, *J. Vac. Sci. Technol. B* **10**, 1898 (1992).
- <sup>10</sup>A. J. van Bommel and J. E. Crombeen, *Surf. Sci.* **76**, 499 (1978).
- <sup>11</sup>L. J. Brillson, *Surf. Sci. Rep.* **2**, 123 (1982).
- <sup>12</sup>I. M. Vitomirov, A. D. Raisanen, L. J. Brillson, P. D. Kirchner, G. D. Pettit, and J. M. Woodall, *Solid State Commun.* **84**, 61 (1992).
- <sup>13</sup>I. M. Vitomirov, A. D. Raisanen, and L. J. Brillson (unpublished).
- <sup>14</sup>W. Ranke, *Phys. Rev. B* **27**, 7807 (1983).
- <sup>15</sup>D. W. Niles, M. Tang, H. Höchst, and G. Margaritondo, *J. Vac. Sci. Technol. A* **5**, 2057 (1987).
- <sup>16</sup>J. J. Joyce, M. Dei Giudice, and J. H. Weaver, *J. Electron Spectrosc. Relat. Phenom.* **49**, 31 (1989).
- <sup>17</sup>G. Le Lay, D. Mao, A. Khan, Y. Hwu, and G. Margaritondo, *Phys. Rev. B* **43**, 14 301 (1991).
- <sup>18</sup>M. D. Pashley, K. W. Haberern, W. Friday, J. M. Woodall, and P. D. Kirchner, *Phys. Rev. Lett.* **60**, 2176 (1988); M. D. Pashley, *Phys. Rev. B* **40**, 10 481 (1989).
- <sup>19</sup>D. K. Biegelsen, R. D. Bringans, J. E. Northrup, and L.-E. Swartz, *Phys. Rev. B* **41**, 5701 (1990).
- <sup>20</sup>*The NBS Tables of Chemical Thermodynamic Properties*, edited by D. Wagman [*J. Phys. Chem. Ref. Data* **11**, Suppl. 2 (1982)].
- <sup>21</sup>M. C. Schabel, I. M. Vitomirov, G. D. Waddill, and J. H. Weaver, *J. Electron Spectrosc. Relat. Phenom.* **56**, 211 (1991).
- <sup>22</sup>J. J. Yeh and I. Lindau, *At. Nucl. Data Tables* **32**, 1 (1985).
- <sup>23</sup>B. W. Liang and C. W. Tu, *J. Appl. Phys.* **72**, 2806 (1992).